PCCP



COMMUNICATION

View Article Online



Cite this: Phys. Chem. Chem. Phys., 2018, 20, 14287

Received 17th January 2018, Accepted 2nd May 2018

DOI: 10.1039/c8cp00384i

rsc.li/pccp

Reductive defluorination of graphite monofluoride by weak, non-nucleophilic reductants reveals low-lying electron-accepting sites†

Yijun Liu, D‡a_Benjamin W. Noffke, Xinfeng Gao, Yaroslav Lozovyi, Yi Cui, bc Yongzhu Fu, 📵 d Krishnan Raghavachari, a Allen R. Siedle* and Liang-shi Li*

Graphite monofluoride (GF) can undergo reductive defluorination in the presence of weak, non-nucleophilic reductants. This leads to a new approach to GF-polyaniline composites as cathode materials for significantly improving the discharge capacity of primary lithium batteries. We postulate that the reduction is mediated by residual π -bonds in GF.

Conversion between sp²- and sp³-hybridized carbon is a common theme in modification of the electrical, optical, chemical, or dispersion properties of graphitic carbon materials. Among graphite-derived sp³-carbon compounds, graphite monofluoride (GF, stoichiometry CF₁), with a fluorine atom covalently linked to each carbon atom, is of particular interest.2 GF can be reduced and defluorinated at room temperature by lithium to recover sp²-carbon, along with the formation of LiF.³ Because of its large thermodynamic driving force, this reaction has been commercially applied to make lithium primary batteries with the highest energy-density among all lithium-based batteries.3,4 In addition, the reductive defluorination of GF and graphene fluoride, the fluorinated counterpart of graphene,⁵ has been recently applied to make graphene nanostructures with controlled dimensions and bandgap.6 Therefore, an improved understanding of the reductive defluorination of GF can lead to novel processes to control the reactions and may have practical significance.

Because of its structural complexity, understanding of the properties of GF is largely based on theoretical calculations with certain assumptions applied regarding its structure.⁷ For example,

GF is generally considered as stacks of two-dimensional arrays of edge-sharing cyclohexyl rings with a fluorine atom linked to each carbon atom. DFT calculations on such structures have shown that GF has the top of the valence band at approximately 7.7 eV below vacuum and a valence-conduction bandgap of approximately 7.4 eV, almost independent of the conformation of the cyclohexyl rings (i.e., chair, boat, etc.).8 This suggests that GF has a very low electron affinity close to 0.3 eV and explains the need for strong reductants, such as alkaline metals, for reductive defluorination of GF, unless the reductants are simultaneously capable of nucleophilic attack (e.g., hydrazine and iodide). 4,5,9 Here we report new findings on reductive defluorination of GF by weak, nonnucleophilic, reductants. The observations have been applied to make a novel GF-polyaniline composite, leading to improved discharge capacity in primary lithium batteries. In addition, we suggest that residual π -bonds in GF are the electron-accepting sites for triggering the defluorination reaction.

As mentioned above, we recently found, unexpectedly, that GF can be reduced by weak reductants with negligible nucleophilicity, indicating its high oxidizing power and the existence of low-lying electron-accepting states (vide infra). This is indicated by a color change when N,N,N',N'-tetramethyl-p-phenylenediamine (TMPD, known as Wurster's blue), a weak non-nucleophilic reductant, was added to a GF suspension in acetonitrile at room temperature. Within a few seconds, the liquid phase turned blue, a characteristic color of radical cations of TMPD (i.e., TMPD•+), suggesting the oxidation of TMPD and the reduction of GF (Fig. 1a). This was subsequently confirmed by electron paramagnetic resonance spectroscopy (EPR) measurements at 298 K which revealed a hyperfine splitting pattern (Fig. 1b) identical to that reported for the TMPD radical cations. 10

GF can be reduced by even weaker reductants, though at decreased reaction rates. TMPD has a standard potential of $E^0 = +0.41 \text{ V } \text{vs.}$ the standard hydrogen electrode (SHE)¹¹ in acetonitrile (or 4.85 V vs. the vacuum level12). GF can oxidize other weak reductants, such as decamethylferrocene (FeCp2*, E^0 = +0.12 V vs. SHE), ¹³ tetrathiafulvalene (TTF, E^0 = +0.56 V vs. SHE), ¹⁴ and decamethylosmocene (OsCp₂*, $E^0 = +0.64 \text{ V} \text{ vs. SHE}$). ¹⁵

^a Department of Chemistry, Indiana University, Bloomington, Indiana, 47405, USA. E-mail: arsiedle@indiana.edu, li23@indiana.edu

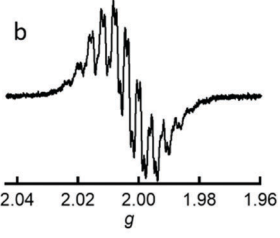
^b Department of Mechanical Engineering, Indiana University-Purdue University Indianapolis, Indianapolis, Indiana, 46202, USA

^c School of Mechanical Engineering, Purdue University, West Lafayette, Indiana,

^d College of Chemistry and Molecular Engineering, Zhengzhou University, Zhengzhou 450001, P. R. China

[†] Electronic supplementary information (ESI) available: Experimental details, supplementary results, and theoretical calculations. See DOI: 10.1039/c8cp00384j ± Current address: National Key Laboratory of Science and Technology on Power Sources, Tianjin Institute of Power Sources, Tianjin 300384, P. R. China.

2.016 2.012 2.008



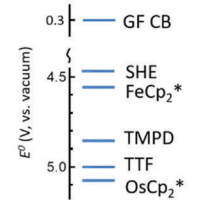


Fig. 1 Reduction of GF by weak reductants. (a) Color before (left) and after (right) TMPD is added to GF. The liquid is acetonitrile. (b) The EPR spectrum of TMPD*+ at 298 K as a result of oxidation of TMPD by GF. (c) The EPR spectrum of TTF⁺⁺ at 205 K as a result of oxidation of TTF by GF. (d) Standard reduction potentials of the reductants in acetonitrile vs. the vacuum level. For comparison, the position of the bottom of the calculated conduction band (CB) of GF is also shown.8

Under the same reaction conditions as those for TMPD described above, for FeCp2* the oxidation product can be observed within seconds with UV-absorption spectra (ESI,† Fig. S1), but for TTF it takes minutes for TTF^{•+} to be observed with EPR (Fig. 1c). OsCp₂*, an even weaker reductant, was barely able to reduce GF even days after mixing (ESI,† Fig. S1). Fig. 1d summarizes the standard redox potentials of the reductants studied, together with the position of the bottom of the calculated conduction band of defect-free GF for comparison.8 Since there is a large discrepancy in the electron affinity of GF and the reduction potentials of the reductants, the observed reduction can only be explained by other acceptor states in GF (vide infra).

Meanwhile, reduction of GF by weak reductants releases fluoride to the liquid phase of the reaction mixtures. For example, Fig. 2a shows the fluorine-NMR spectrum of the supernatant of the reaction mixtures with TMPD, revealing the appearance of soluble fluorine-containing species after the reaction. The chemical shifts of the peaks $(-130 \text{ and } -152 \text{ ppm}, \text{ relative to } \text{CFCl}_3)$ correspond to SiF₆²⁻ and BF₄⁻, respectively, due to corrosion of the borosilicate glass NMR tube by F-. The same results were also observed in reaction mixtures with FeCp₂* or TTF (ESI,† Fig. S2). Furthermore, the solids from the reaction mixture showed decreased fluorine content and formation of sp²-hybridized carbon. X-ray photoelectron spectroscopy (XPS) measurements of the solid product obtained with TMPD showed F/C = 0.71 after a week, significantly lower than the starting F/C atomic ratio of 1.0 (ESI,† Table S1). The Raman spectrum of this material (514.5 nm excitation, Fig. 2b) showed new peaks at 1330 (FWHM 50) and 1600 (FWHM 30) cm⁻¹ (intensity ratio $\sim 1.1:1$). This can be interpreted as either graphene with an extremely high defect density¹⁶ or a continuous network of C=C bonds, indicating the conversion of sp³-carbon in GF to sp²-carbon. This is consistent with the color change of the solids from the original pale gray to black, as can be visualized in Fig. 1a.

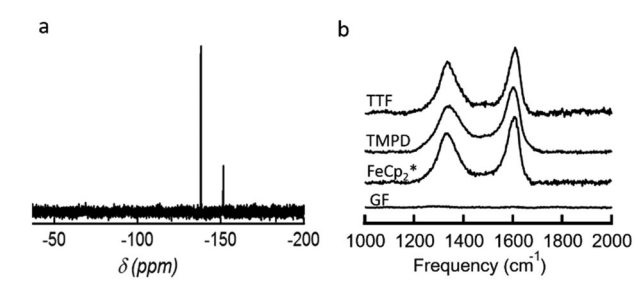


Fig. 2 Defluorination of GF by weak reductants. (a) An F-NMR spectrum of the supernatant from the GF-TMPD reaction mixture. (b) Raman spectra (514.5 nm excitation) of the solid products after GF was exposed to various reductants compared with that of the starting GF.

However, X-ray diffraction measurements did not reveal any longrange structural order or graphite formation.

The surprising observation of GF reduction by weak reductants prompted us to apply GF as an oxidant for synthetic purposes. In particular, we applied it to make a GF-polyaniline composite material with increased electrical conductivity for the Li/CF_r battery. Graphite fluoride with various fluorine content has important applications as cathode materials for primary batteries.^{3a,4} In particular, the lithium/graphite fluoride (denoted Li/CF_x, 0 < x < 1.5) primary battery employs lithium as the anode, and, because of the light mass and small radii of lithium and fluoride ions, it has one of the highest theoretical specific energies (e.g., 2180 W h kg⁻¹ for x = 1.0) among solid cathode systems. In addition, the Li/CF_r battery has very slow self-discharge ($\sim 0.5\%$ per year) and a very long shelf life (>10 years), making it desirable for devices that require a long battery life such as in cardiac pacemakers as well as in some military, aerospace, and electronic devices. A challenge that limits the application of the Li/CF_x battery has been the poor electrical conductivity of the CF_x cathode.4 This leads to a number of drawbacks such as low output power, heat generation during discharging, etc.

The GF-polyaniline composite material was synthesized by dispersing GF (as-received, stoichiometry CF_{1.1}) in a solution of aniline in an acidified acetonitrile/water mixture, followed by stirring in air for 30 days at room temperature. Similar to the reactions described above, the GF powder turned black, with the supernatant turning violet. The violet color is characteristic of pernigraniline, a highly oxidized form of polyaniline.¹⁷ The solids in the reaction mixture were subsequently washed repetitively to remove unreacted aniline and soluble reaction products until the supernatant appeared colorless. The IR spectra of the solid products in KBr pellets confirmed the presence of polyaniline in the solid products of the GF-aniline reaction (ESI,† Fig. S5). Furthermore, XPS showed that the C/F atomic ratio changed from the original 1/1.1 to 1/0.80 (ESI,† Fig. S4). From the XPS-measured N content, we estimated the weight percentage of polyaniline in the solids to be less than 4%. Therefore, mixing aniline with GF produces sp²-carbon from partial reduction of the GF as well as conjugated polyaniline due to the oxidative polymerization of aniline, both of which could contribute to the electrical conductivity of the composite material. Because electron transfer occurs over a short distance, we speculate

that the polymerization occurs only at the solid/liquid interface, leading to intimate mixing of polyaniline with partially reduced GF. In contrast, in a control experiment, aniline stirred under the same reaction conditions without GF led to a brown solution, characteristic of air-oxidized aniline.18

We subsequently made Li/CF_r coin cells with either GF or the GF-polyaniline composite as the cathode materials and tested their discharge characteristics. For the cathode, either of the two materials were mixed with carbon black, with polyvinylidene fluoride (PVDF) binder at a weight ratio of 85:10:5. A lithium metal sheet was used as the anode and coin cells were assembled under identical conditions (details in the ESI†). Fig. 3a shows the Nyquist plots of the impedance of the cells measured between 200 kHz and 0.1 Hz (black for GF and red for GF-polyaniline). As indicated by the intercepts on the x-axis (i.e., the real part of the impedance, Z'), the cells made with the GF-polyaniline composite have an internal resistance of only a third of that of cells made with GF (6.2 Ω vs. 17.9 Ω). We attribute it to contributions from both the sp²-carbon formed in reduced GF and the polyaniline in the composite, having intimate electrical contact. This leads to superior discharge capacity, as shown in Fig. 3b. At a discharge rate of C/50, cells made with GF-polyaniline yielded a specific capacity of 659 mA h g⁻¹ (for a voltage drop from the initial 2.5 V to 1.5 V). This is significantly higher than 526 mA h g^{-1} for cells made with GF, despite the lower fluorine content in the GF-polyaniline composite.

The facile reduction of GF by the weak, non-nucleophilic reductants raises interesting questions regarding the electron-accepting

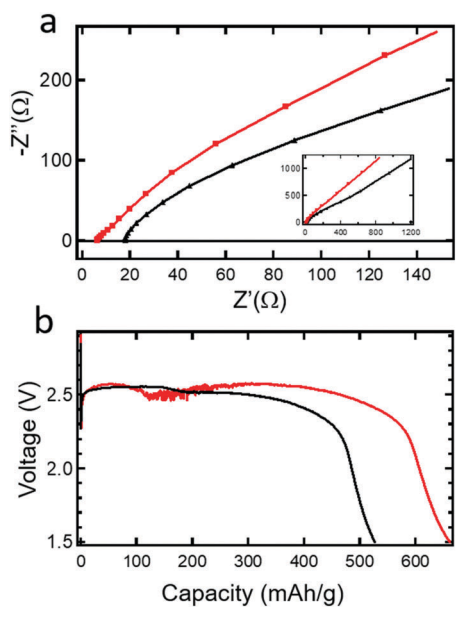


Fig. 3 (a) High-frequency region of the impedance spectra of Li/CF_x batteries made with GF (black) and the GF-polyaniline composite materials (red), respectively, in the cathode. Inset: Full-range spectra measured between 200 kHz and 0.1 Hz. (b) Discharge curves of the Li/CF_x batteries made with GF (black) and the GF-polyaniline composite materials (red), respectively. The discharge rate is C/50. The measurements were stopped when the discharge voltage decreased to 1.5 V from the initial 2.5 V, with a specific capacity of 526 mA h g^{-1} (based on the mass of GF) and 659 mA h g^{-1} (based on the mass of the GF-polyaniline composite used).

states and the defluorination mechanism. Because of the negligible nucleophilicity of the weak reductants studied, in order to effect C-F bond cleavage, clearly the electron-accepting states should have significant orbital overlap with the antibonding (σ^*) orbital of the C-F bond.¹⁹ Fully saturated perfluoroalkanes have electron affinities less than 1 eV,8 which is too low to account for the observed reduction, suggesting the involvement of other structural features that are generally ignored in GF. In particular, residual π -bonds may exist in GF due to incomplete fluorination in production. This is indicated by XPS in the samples we studied (ESI,† Fig. S4), which shows peaks at the same C 1s binding energy as partly reduced GF. In addition, the gray color of GF suggests the existence of extended conjugated C=C bonds. Studies on small molecules have shown that perfluoroalkyl-substituted olefins could have significantly greater electron affinity than perfluoroalkanes or olefins. For example, 1,1,2,2-tetra(trifluoromethyl)ethylene (TTFME) has a reduction potential of -0.61 V vs. SCE (-0.37 V vs. SHE, or 4.1 V below vacuum) in acetonitrile.²⁰

To evaluate the feasibility that the residual -bonds in GF may be responsible for the electron transfer, we calculated the electron affinity of graphene fluoride containing an ethylene moiety. This was done with nanometer-sized graphene fluoride fragments of various sizes (ESI,† e.g., Fig. S6) until the calculated electron affinity remains invariant with increasing size. Our calculations yielded an electron affinity of 3.8 eV, comparable to the experimental value of TTFME within the uncertainty of the calculations.21 The large electron affinity is primarily due to the effective overlap between the π^* orbital and the σ^* orbitals of the β-CF bonds, a phenomenon known as negative anionic hyperconjugation in small-molecule fluorohydrocarbons.²² As a result, the greater electronegativity of the fluorine atoms decreases the energy of the π^* orbital and stabilizes the carbanion. Our estimate of the thermodynamic driving force for the electron transfer from the reductants to GF shows that it is possible through likely an uphill process (see the ESI†). The subsequent elimination of F^- because of the partial occupation of the β -CF σ^* orbitals after reduction of GF,²² together with the large excess of the reductants present, shifts the equilibrium in the direction favoring the reductive defluorination, consistent with our observations. The reduction and defluorination may proceed repetitively, similar to a reaction sequence proposed for the defluorination of perfluorodecalin to yield octafluoronapthalene.²³ Our calculations show that such sequences are energetically feasible (see the ESI†). Defluorination produces either radical species or conjugated alkenes with increasing conjugation length, which have increased the electron affinities and make further reduction more favorable. In addition, extended conjugated C=C bonds that likely preexist in GF as indicated by its gray color can also serve as electron-accepting sites for the reduction. However, we note that due to the complex long-range structures of GF and various bonding conformations possible, our current work only suggests the possible roles of the unsaturated carbon species in reductive defluorination. A detailed reaction mechanism warrants further investigation.

In summary, we show unexpected reductive defluorination of graphite monofluoride (GF) by weak, non-nucleophilic reductants, indicating the presence of low-lying electron-accepting sites.

Furthermore, we could take advantage of the reduction properties of GF to oxidize aniline, a weak reductant, to synthesize GF–polyaniline composites. The use of the composites as cathode materials led to significantly improved discharge capacity of primary lithium batteries. Based on an analysis of the redox energetics, we postulate that the reduction of GF is mediated by residual π -bonds in GF. The hyperconjugation between the π^* orbital and the σ^* orbitals of the β -CF bonds enhances the electron accepting properties of the materials.

Conflicts of interest

The authors have no conflicts to declare.

Acknowledgements

This work is supported by Indiana University and the National Science Foundation (NSF grant CHE-1665427). The XPS measurements were done at the Nanoscale Characterization Facility of Indiana University (NSF grant DMR MRI-1126394).

Notes and references

- (a) D. R. Dreyer, S. Park, C. W. Bielawski and R. S. Ruoff, *Chem. Soc. Rev.*, 2010, 39, 228–240; (b) F. Karlický, K. K. R. Datta, M. Otyepka and R. Zbořil, *ACS Nano*, 2013, 7, 6434–6464; (c) M. Pumera and C. H. A. Wong, *Chem. Soc. Rev.*, 2013, 42, 5987–5995.
- 2 O. Ruff and O. Bretschneider, Z. Anorg. Allg. Chem., 1934, 217, 1-18.
- 3 (a) M. S. Whittingham, J. Electrochem. Soc., 1975, 122, 526–527; (b) H. Touhara, H. Fujimoto, N. Watanabe and A. Tressaud, Solid State Ionics, 1984, 14, 163–170.
- 4 Q. Zhang, K. J. Takeuchi, E. S. Takeuchi and A. C. Marschilok, *Phys. Chem. Chem. Phys.*, 2015, 17, 22504–22518.
- (a) J. T. Robinson, J. S. Burgess, C. E. Junkermeier, S. C. Badescu, T. L. Reinecke, F. K. Perkins, M. K. Zalalutdniov, J. W. Baldwin, J. C. Culbertson, P. E. Sheehan and E. S. Snow, *Nano Lett.*, 2010, 10, 3001–3005; (b) R. R. Nair, W. Ren, R. Jalil, I. Riaz, V. G. Kravets, L. Britnell, P. Blake, F. Schedin, A. S. Mayorov, S. Yuan, M. I. Katsnelson, H.-M. Cheng, W. Strupinski, L. G. Bulusheva, A. V. Okotrub, I. V. Grigorieva, A. N. Grigorenko, K. S. Novoselov and A. Geim, *Small*, 2010, 6, 2877–2884; (c) R. Zbořil, F. Karlický, A. B. Bourlinos, T. A. Steriotis, A. K. Stubos, V. Georgakilas, K. Šafářová, D. Jančík, C. Trapalis and M. Otyepka, *Small*, 2010, 6, 2885–2891.
- 6 W.-K. Lee, M. Haydell, J. T. Robinson, A. R. Laracuente, E. Cimpoiasu, W. P. King and P. E. Sheehan, *ACS Nano*, 2013, 7, 6219–6224.

- 7 (a) W. Rüdorff and G. Rüdorff, Z. Anorg. Chem., 1947, 253, 281–296; (b) L. B. Ebert, J. I. Brauman and R. A. Huggins, J. Am. Chem. Soc., 1974, 96, 7841–7842; (c) Y. Kita, N. Watanabe and Y. Fujii, J. Am. Chem. Soc., 1979, 101, 3832–3841; (d) H. Touhara, K. Kadono, Y. Fujii and N. Watanabe, Z. Anorg. Allg. Chem., 1987, 544, 7–20; (e) J.-C. Charlier, X. Gonze and J.-P. Michenaud, Phys. Rev. B: Condens. Matter Mater. Phys., 1993, 47, 16162–16168; (f) S. S. Han, T. H. Yu, B. V. Merinov, A. C. T. van Duin, R. Yazami and W. A. I. Goddard, Chem. Mater., 2010, 22, 2142–2154.
- 8 O. Leenaerts, H. Peelaers, A. D. Hernández-Nieves, B. P. Partoens and F. M. Peeters, *Phys. Rev. B: Condens. Matter Mater. Phys.*, 2010, 82, 195436.
- 9 (a) R. Zbořil, F. Karlický, A. B. Bourlinos, T. A. Steriotis, A. K. Stubos, V. Georgakilas, K. Šafářová, D. Jančík, C. Trapalis and M. Otyepka, *Small*, 2010, 6, 2885–2891; (b) K. E. Whitener Jr., R. Stine, J. T. Robinson and P. E. Sheehan, *J. Phys. Chem. C*, 2015, 119, 10507–10512.
- 10 T. R. Tuttle, J. Chem. Phys., 1959, 30, 331.
- 11 M. Jonsson, A. Houmam, G. Jocys and D. D. M. Wayner, J. Chem. Soc., Perkin Trans. 2, 1999, 425–429.
- 12 S. Trasatti, Pure Appl. Chem., 1986, 58(7), 955-966.
- 13 P. Zanello, A. Cinquantini, S. Mangani, G. Opromolla, L. Pardi, C. Janiak and M. D. Rausch, *J. Organomet. Chem.*, 1994, 471, 171–177.
- 14 (a) P. R. Ashton, V. Balzani, J. Becher, A. Credi, M. C. T. Fyfe, G. Mattersteig, S. Menzer, M. B. Nielsen, F. M. Raymo, J. F. Stoddart, M. Venturi and D. J. Williams, *J. Am. Chem. Soc.*, 1999, 121, 3951–3957; (b) F. Wudl, G. M. Smith and E. J. Hufnagel, *Chem. Commun.*, 1970, 1453–1454.
- 15 A. Pedersen, V. Skagestad and M. Tilset, *Acta Chem. Scand.*, 1995, 49, 632–635.
- 16 R. Beams, L. G. Cancado and L. Novotny, J. Phys.: Condens. Matter, 2015, 27, 083002.
- 17 Y. Sun, A. G. MacDiarmid and A. J. Epstein, *J. Chem. Soc., Chem. Commun.*, 1990, 529–531.
- 18 R. Konaka, K. Kururna and S. Terabe, *J. Am. Chem. Soc.*, 1968, **90**, 1801–1806.
- 19 (a) Y. A. Maletin and R. D. Cannon, *Theor. Exp. Chem.*, 1998,
 34, 57–68; (b) H. Amii and K. Uneyama, *Chem. Rev.*, 2009,
 109, 2119–2183.
- 20 C. Corvaja, G. Farnia, G. Formenton, W. Navarrini, G. Sandona and V. Tortelli, *J. Phys. Chem.*, 1994, **98**, 2307–2313.
- 21 B. W. Noffke, Q. Li, K. Raghavachari and L.-S. Li, *J. Am. Chem. Soc.*, 2016, **138**, 13923–13929.
- 22 P. v. R. Schleyer and A. J. Kos, *Tetrahedron*, 1983, 39, 1141–1150.
- 23 G. Sandford, Tetrahedron, 2003, 59, 437-454.